Available online at www.sciencedirect.com
SCIENCE DIRECT®
ELSEVIER
Physica B 340–342 (2003) 697–700
PHYSICA B
www.elsevier.com/locate/physb

Local vibrational modes of bond-centered H in ^{28}Si, ^{29}Si, and ^{30}Si crystals

R.N. Pereira[a,*], T. Ohya[b], K.M. Itoh[b], B. Bech Nielsen[a]

[a] *Department of Physics and Astronomy, University of Aarhus, DK-8000 Aarhus, Denmark*
[b] *Department of Physics, Keio University, Kanagawa, Japan*

Abstract

The local vibrational mode of positively charged bond-centered hydrogen (H_{BC}^{+}) has been investigated in Si crystals enriched with ^{28}Si, ^{29}Si, or ^{30}Si isotopes. Protons and deuterons were implanted into each sample at temperatures below 20 K, and in-situ-type infrared absorption measurements were subsequently performed at 8 K. The isotope shifts observed for the hydrogen and deuterium modes display opposite behavior with increasing mass of the silicon isotope. This behavior cannot be accounted for with a purely harmonic potential. We apply a simple model based on the linear molecule Si–H–Si, where the potential associated with the stretching of each Si–H bond is approximated by the Morse potential. The local mode frequencies and the isotope shifts obtained with our model are in excellent agreement with those observed.

PACS: 61.72.Tt; 63.20.Pw; 74.62.Dh; 78.30.Am

Keywords: Silicon; Hydrogen; FTIR; Anharmonicity

---

1. Introduction

Hydrogen can influence the electronic performance of crystalline silicon due to its ability to interact with lattice imperfections. The local vibrational modes (LVMs) of point defects in solids have traditionally been described with purely harmonic potentials, neglecting any anharmonic effects. Although this approach may be valid for many impurity centers in silicon, it is inadequate to describe the LVMs of light elements like hydrogen. In this context, bond-centered hydrogen (H_{BC}^{+}) in silicon is an obvious candidate for a detailed study, since its structure is well established and the defect has been characterized in great detail [1–7]. Positively charged H_{BC}^{+} gives rise to an absorbance line at 1998 cm^{-1} in Si, whereas the corresponding deuterium line appears at 1448 cm^{-1} [3].

Isotopically enriched silicon crystals implanted with proton (or deuterium) are studied by Fourier-transform infrared absorption. The frequency shifts of the H_{BC}^{+} (or D_{BC}^{+}) LVM when the silicon mass is changed are investigated. A theoretical model that accounts for the experimental data is introduced and discussed.

---

*Corresponding author. Tel.: +45-894-23-723; fax: +45-86120740.
E-mail address: pereira@phys.au.dk (R.N. Pereira).

0921-4526/$ - see front matter © 2003 Published by Elsevier B.V.
doi:10.1016/j.physb.2003.09.168

2. Experimental details

In this work Si crystals grown by the Czochralski method were used that were isotopically enriched with ^{28}Si (enriched to 99.93%), ^{29}Si (enriched to 97.10%), and ^{30}Si (enriched to 99.75%). The samples were mounted in a cryostat placed inside a vacuum chamber, which in turn was connected to the accelerator beam line. The samples were implanted with protons (or deuterons) with different energies in the range 5–10 MeV at temperatures below 20 K. The energy step and doses at each implantation energy were adjusted to result in a nearly homogeneous hydrogen (or deuterium) concentration of 10^{18}–10^{19} cm^{-1} in the range from 150 to 550 μm below the surface. After the implantation, the cryostat was moved to the infrared spectrometer, while keeping the sample temperature below 20 K.

The infrared absorption measurements were carried out with a Nicolet, System 800, Fourier-transform spectrometer, equipped with a glowbar light source, a Ge–KBr beam splitter, and a mercury–cadmium–telluride detector. The spectra were recorded at ~8 K with an apodized resolution of 0.25 cm^{-1}.

3. Experimental results

In Fig. 1 sections of the absorbance spectra measured on the ^{28}Si, ^{29}Si, and ^{30}Si samples after low temperature implantation of protons or deuterons are shown. The absorbance lines shown in the plots represent the excitation of the stretch mode of H_{BC}^{+} and D_{BC}^{+} in Si. The assignment of the observed lines to the 1998-cm^{-1} and 1448-cm^{-1} LVMs of H_{BC}^{+} and D_{BC}^{+}, respectively, is confirmed by their frequencies and by their annealing behavior. An example of the annealing behavior is shown in Fig. 2. As can be seen from the figure, the line anneals out after heat treatment at 200 K as reported previously for H_{BC}^{+} (and D_{BC}^{+}) [3]. In order to achieve an accurate determination of the frequencies of the modes for the different Si isotopes, the experimental lineshapes were fitted with Lorentzian profiles. The resulting line positions are also given in Fig. 1.

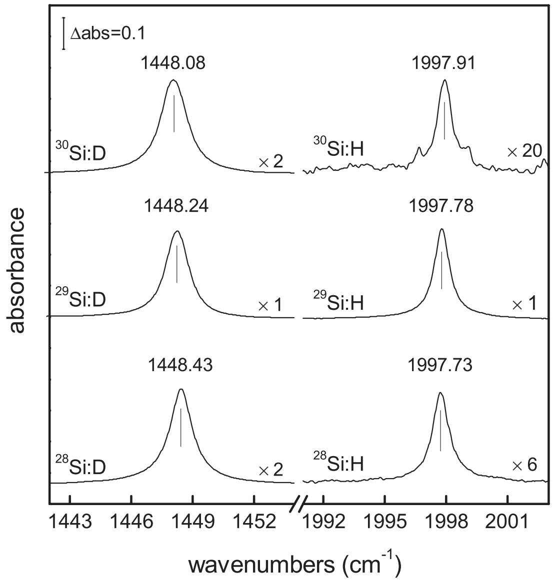

Fig. 1. Sections of absorbance spectra measured at ~8 K on ^{28}Si, ^{29}Si, and ^{30}Si crystals implanted with protons or deuterons. The plots show the isotope shifts induced on the 1998-cm^{-1} (or 1448-cm^{-1}) stretch mode of H_{BC}^{+} (or D_{BC}^{+}).

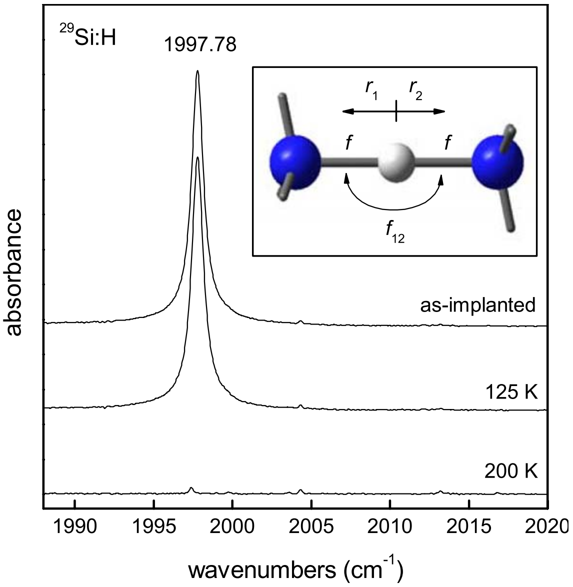

Fig. 2. Annealing behavior of the H_{BC}^{+} local mode in the proton-implanted ^{29}Si sample. The inset shows a sketch of the Si–H–Si triatomic unit used to model the vibrational properties of the defect.

As can be seen from the figure, the shifts in the mode frequency were produced by changing the Si-isotope display opposite behavior for H_{BC}^{+} and D_{BC}^{+}. The frequency of the H_{BC}^{+} mode increases when the Si mass increases, whereas the D_{BC}^{+} mode decreases in frequency when the Si mass increases. This is a puzzling effect which contradicts conventional wisdom that the frequency decreases when the mass of the oscillator increases.

4. Model of the bond-centered hydrogen defect

The theoretical model introduced here is based on the Si–H–Si molecular unit shown in the inset of Fig. 2, where r_1 and r_2 denote the stretching of the two bonds. Assuming anharmonic potential for each of the two coupled Si–H oscillators the frequency of the Si–H stretch mode is given by

$$\omega_{\text{harm}} = \sqrt{\frac{f - f_{12}}{m_{\text{eff}}}}, \tag{1}$$

where the force constant for each bond is denoted by f, whereas f_{12} is the harmonic coupling constant between the two Si–H bonds, and the effective mass of the oscillator m_{eff} is given by

$$\frac{1}{m_{\text{eff}}} = \frac{2}{m_{\text{H}}} + \frac{1}{\chi m_{\text{Si}}}. \tag{2}$$

m_{H} and m_{Si} denote the hydrogen and Si atomic masses, respectively, and χ is a factor that accounts for the coupling with the lattice [8]. Considering that the potential energy for given values of r_1 and r_2 is independent of the isotopic composition of the system, i.e., that the parameters f, f_{12}, and χ are the same for the different isotopic configurations of the defect, Eq. (1) predicts a decrease of the mode frequency as the Si mass increases for both H_{BC}^{+} and D_{BC}^{+}. In contrast to this, the peak frequencies of the H_{BC}^{+} mode increase slightly with the increasing mass of Si, whereas the shift of the D_{BC}^{+} mode as the Si mass increases is negative (see Fig. 1). Such a behavior cannot be described by a vibrational model based on a purely harmonic potential, which demonstrates the need to include anharmonic effects.

The Morse potential has often been applied to account for anharmonicity in the vibration of diatomic molecules [9]. If we assume that the two Si–H bonds may be well described by such a potential, our model Hamiltonian is

$$\mathscr{H} = -\frac{\hbar^2}{2}\sum_{i,j} G_{ij}\frac{\partial^2}{\partial r_i r_j} + D_1[1 - \mathrm{e}^{-\alpha_1 r_1}]^2 + D_2[1 - \mathrm{e}^{-\alpha_2 r_2}]^2 + f_{12} r_1 r_2, \tag{3}$$

where α_1, D_1, α_2, and D_2 are the Morse potential parameters and G_{ij} is the ijth element of the so-called **G** matrix [10]. If the two terms of the Morse potential are expanded to fourth order and we take into account that by symmetry $\alpha_1 = \alpha_2 = \alpha$ and $D_1 = D_2 = D$, the Hamiltonian (3) reads

$$\mathscr{H}_{\text{harm}} = -\frac{\hbar^2}{2}\sum_{i,j} G_{ij}\frac{\partial^2}{\partial r_i r_j} + \frac{1}{2}f(r_1^2 + r_2^2) + f_{12} r_1 r_2 + f_3(r_1^3 + r_2^3) + f_4(r_1^4 + r_2^4), \tag{4}$$

$$\text{with } f = 2D\alpha^2,\ f_3 = -D\alpha^3 \quad \text{and} \quad f_4 = \tfrac{7}{12}D\alpha^4. \tag{5}$$

The anharmonic energy correction is calculated by perturbation theory as the sum of the second-order correction of the cubic terms and the first-order correction of the quartic terms. We find that the frequency correction to the harmonic frequency ω_{harm} may be written as

$$\omega_{\text{anharm}} = \frac{A}{m_{\text{eff}}} + \frac{B}{\sqrt{m_{\text{Si}} m_{\text{eff}}}} + \omega_r, \tag{6}$$

where

$$A = -\frac{3\hbar}{2}\left(\frac{3f_3^2}{f^2 - f_{12}^2} - \frac{f_4}{f - f_{12}}\right), \tag{7}$$

$$B = -\frac{3\hbar}{4}\left(\frac{3f_3^2}{(f + f_{12})\sqrt{f^2 - f_{12}^2}} - \frac{2f_4}{\sqrt{f^2 - f_{12}^2}}\right), \tag{8}$$

$$\omega_r = -\frac{9\hbar}{4}\left(\frac{f_3^2}{m_{\text{eff}}(f^2 - f_{12}^2) + 2\sqrt{m_{\text{Si}}\, m_{\text{eff}}}(f - f_{12})\sqrt{f^2 - f_{12}^2}}\right). \tag{9}$$

With $\chi = 1$ the frequencies of the hydrogen stretch mode were calculated for the six isotopic configurations of the defect, and the optimum parameters α, D, and f_{12} were determined by minimizing the sum of the square of the differences between the calculated and the observed frequencies (Table 1). Our model reproduces the opposite isotope shifts with the increasing Si mass observed for the H_{BC}^{+} and D_{BC}^{+} centers. Moreover, the model reproduces the frequencies of the six defect configurations to within 0.11 cm^{-1}. In Fig. 3 the contributions of the different anharmonic terms in Eq. (6) to the isotope shift (ω_{30}-ω_{28}) when ^{28}Si is substituted by ^{30}Si are shown. Although the signs of the different contributions are the same for H_{BC}^{+} and D_{BC}^{+} the relative magnitudes of the different terms result in an overall positive isotope shift for H_{BC}^{+} and a negative shift for D_{BC}^{+}. The two dominating contributions to ω_{30}-ω_{28} are the harmonic frequency shift $\Delta\sqrt{\frac{f-f_{12}}{m_{\mathrm{eff}}}}$, which is negative, and $\Delta\frac{B}{\sqrt{m_{\mathrm{Si}}m_{\mathrm{eff}}}}$, which is positive. The magnitude of the negative shift from the harmonic term is higher for D_{BC}^{+} than for H_{BC}^{+}, whereas the positive shift due to the $\frac{B}{\sqrt{m_{\mathrm{Si}}m_{\mathrm{eff}}}}$ term is greater for hydrogen than for Si. It is the balance between these two contributions that results in an overall positive isotope shift for H_{BC}^{+} and a negative shift for D_{BC}^{+}.

Table 1
Comparison between the calculated model frequencies (cm^{-1}) and those observed for H_{BC}^{+} and D_{BC}^{+} in Si. The model frequencies are calculated using the best-fit parameters $\alpha = 0.413010$ (Å^{-1}), $D = 12.7406$ (eV), and $f_{12} = -4.09272$ (eV Å^{-2})

Isotope configuration	$\omega^{1}_{\mathrm{harm}}$	$\omega^{1}_{\mathrm{anharm}}$	$\omega^{1}_{\mathrm{model}}$	ω_{obs}	$\omega_{\mathrm{obs}} - \omega_{\mathrm{model}}$
^{28}Si–H–^{28}Si	2153.19	−155.54	1997.64	1997.73	0.09
^{29}Si–H–^{29}Si	2152.52	−154.71	1997.81	1997.78	−0.03
^{30}Si–H–^{30}Si	2151.91	−153.93	1997.98	1997.91	−0.07
^{28}Si–D–^{28}Si	1536.51	−87.96	1448.54	1448.43	−0.11
^{29}Si–D–^{29}Si	1535.58	−87.34	1448.24	1448.24	0.00
^{30}Si–D–^{30}Si	1534.73	−86.76	1447.97	1448.08	0.11

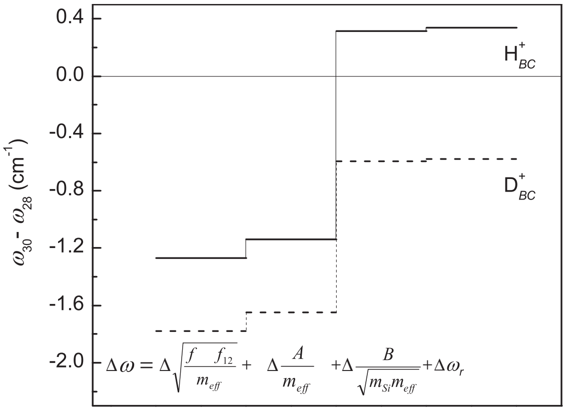

Fig. 3. Evolution of the isotope shift ω_{30}-ω_{28} for H_{BC}^{+} (solid line) and D_{BC}^{+} (dashed line) as the anharmonic correction terms, given by Eq. (6), are sequentially added to the harmonic frequency shift $\Delta\omega_{\mathrm{harm}}$.

5. Conclusion

In this work, the frequencies of H_{BC}^{+} and D_{BC}^{+} in ^{28}Si, ^{29}Si, and ^{30}Si crystals have been identified. A peculiar opposite frequency shift for the H_{BC}^{+} and D_{BC}^{+} LVMs is observed when the Si mass is increased. A detailed vibrational model demonstrates that the effect is caused by anharmonic effects.

Acknowledgements

This work has been supported by the Danish National Research Foundation through Aarhus Center for Advanced Physics (ACAP). R.N.P. thank the ECCN Network for financial support.

References

[1] H.J. Stein, Phys. Rev. Lett. 43 (1979) 1030.
[2] B. Holm, K. Bonde Nielsen, B. Bech Nielsen, Phys. Rev. Lett. 66 (1991) 2360.
[3] M. Budde, Ph.D. Thesis, Aarhus University, Aarhus, Denmark, 1998.
[4] K. Bonde Nielsen, B. Bech Nielsen, J. Hansen, E. Andersen, J.U. Andersen, Phys. Rev. B 60 (1999) 1716.
[5] M. Budde, G. Lüpke, C. Parks Cheney, N.H. Tolk, L.C. Feldman, Phys. Rev. Lett. 85 (2000) 1452.
[6] M. Budde, C. Parks Cheney, G. Lüpke, N.H. Tolk, L.C. Feldman, Phys. Rev. B 63 (2001) 195203.
[7] S.K. Estreicher, Mater. Sci. Eng. Rep. R14 (1995) 319.
[8] R.C. Newman, Physica B 170 (1991) 409.
[9] P.M. Morse, Phys. Rev. 34 (1929) 57.
[10] E. Bright Wilson, J.C. Decius, Paul C. Cross, Molecular Vibrations: The Theory of Infrared and Raman Vibrational Spectra, Dover, New York, USA, 1980.